Chapter 6
Long-Range Lipid-Water Interaction as Observed by ATR-FTIR Spectroscopy

Zoran Arsov

Abstract It is commonly assumed that the structure of water at a lipid-water interface is influenced mostly in the first hydration layer. However, recent results from different experimental methods show that perturbation extends through several hydration layers. Due to its low light penetration depth, attenuated total reflection Fourier transform infrared (ATR-FTIR) spectroscopy is specifically suited to study interlamellar water structure in multibilayers. Results obtained by this technique confirm the long-range water structure disturbance. Consequently, in confined membrane environments nearly all water molecules can be perturbed. It is important to note that the behavior of confined water molecules differs significantly in samples prepared in excess water and in partially hydrated samples. We show in what manner the interlamellar water perturbation is influenced by the hydration level and how it is sequentially modified with a step-by-step dehydration of samples either by water evaporation or by osmotic pressure. Our results also indicate that besides different levels of hydration the lipid-water interaction is modulated by different lipid headgroups and different lipid phases as well. Therefore, modification of interlamellar water properties may clarify the role of water-mediated effects in biological processes.

Keywords ATR-FTIR • Lipid bilayers • Interlamellar water • Excess water • Long-range water structure effect • Water-mediated biological processes

6.1 Introduction

Hydration dynamics and lipid-water interaction strength are closely related to molecular organization and properties of lipids. Since biological membranes play a major role in many cellular processes, they depend on the level of hydration and the structural properties of water molecules at the membrane surface (Fitter et al. 1999; Tamm and Han 2000). Therefore, we have to leave behind the perception

Z. Arsov (✉)
Laboratory of Biophysics, Department of Solid State Physics,"Jozef Stefan" Institute, Jamova 39, SI-1000 Ljubljana, Slovenia
e-mail: zoran.arsov@ijs.si

E.A. Disalvo (ed.), *Membrane Hydration*, Subcellular Biochemistry 71,
DOI 10.1007/978-3-319-19060-0_6

that the influence of water on biological processes is negligible (Chaplin 2006). In recent years, numerous experimental and theoretical evidences were compiled for a substantial role of water in the regulation of biological functions.

Water confined in narrow spaces, e.g. between two opposing lipid membranes, may no longer resemble bulk water. It may be much more viscous, bound to membrane surfaces, etc. (N. of E. * see Chap. 7) During interaction between membranes, water is usually not completely expelled from the confined space, but partly remains present and is involved in the interaction (Ball 2008a). Thus, biological function depends on a delicate interplay between two previously regarded distinct entities: the biomolecule, e.g. a lipid molecule, and its water-based environment (Ball 2008b). Consequently, we have to assign a structural and functional role to the membrane hydration water (Jendrasiak 1996; Milhaud 2004; Disalvo et al. 2008).

In this respect, the hydration force is an important component of the forces operating between phospholipid membranes in water or aqueous solutions. It results from restructuring of interlamellar water with respect to bulk water (Rand and Parsegian 1989; McIntosh and Simon 1994). Accordingly, it is important to understand how lipid bilayers influence the network of water molecules in their vicinity.

Different experimental methods can be used to extract information on the structure and dynamics of water in lipid-water systems, such as nuclear magnetic resonance (NMR) spectroscopy (Finer and Darke 1974; Faure et al. 1997; Kodama et al. 2004), neutron scattering (Kiselev et al. 1999; Fitter et al. 1999), surface force measurements (Higgins et al. 2006; Fukuma et al. 2007), calorimetry (Kodama et al. 2001; Lefèvre et al. 2002; Wennerström and Sparr 2003), fluorescence methods (Parasassi et al. 1991; Beranová et al. 2012), terahertz spectroscopy (Tielrooij et al. 2009; Hishida and Tanaka 2011), and vibrational spectroscopy or their combination (Pfeiffer et al. 2013). (N.of E. * see also Chap. 4). Vibrational spectroscopy is especially suited to probe hydrogen bonding (H-bonding) characteristics of water. In this regard, the shape and position of the hydroxyl (OH) stretching band of water can be used to detect different species of water as well as to examine the water H-bonding network.

There have been several attempts to probe the effect of lipid bilayers on the structure and dynamics of water molecules by infrared (IR) spectroscopy (Grdadolnik et al. 1994; Pohle et al. 1998; Volkov et al. 2007a; Binder 2007). However, these studies were performed on partially hydrated samples, where one gets information only about water located closely to lipid molecules. On the other hand, we are also interested to know whether lipids have any effect on the structure of water distant from the membrane. It can be safely assumed that water molecules that directly interact with lipid molecules are not bulk-like, as this interaction inevitably disturbs their three-dimensional H-bonded network (Ball 2008a). What about water molecules farther away from the membrane? How far does the influence of the membrane surface propagate into the water and what are the manifestations of such propagation (Berkowitz and Vácha 2012)?

The only way to answer these questions is to conduct experiments on lipid samples that are fully hydrated, i.e. hydrated beyond the excess water point, rather

than on incompletely hydrated samples. To our knowledge, we were the first to report about the effect on the shape of the OH stretching band measured by attenuated total reflection Fourier transform infrared (ATR-FTIR) spectroscopy on lipid multibilayers prepared in excess water (Arsov and Quaroni 2007; Štrancar and Arsov 2008). The OH stretching band shift to higher frequencies reflected putative weakening of H-bonding in interlamellar water compared to usual strengthening for hydration water directly interacting with lipids. These findings are supported by similar results obtained in studies on lipid membranes prepared in excess water with Raman spectroscopy (Lafleur et al. 1989) and coherent anti-Stokes Raman scattering (CARS) microscopy (Cheng et al. 2003; Wurpel and Müller 2006). To permit direct comparison of the effect on the water structure for samples prepared in excess water and for partially hydrated samples we set to design a single experiment to test the influence of different lipid hydration levels. In addition, such experiment allows studying the corresponding impact of lipid composition/headgroup, lipid phases, and lipid phase transitions.

The aim of this contribution is to show that the structure of the hydration water is modified not only for interfacial water or the first hydration water layer but even beyond. We argue that this reflects a possible long-range lipid-water interaction, which could have implications for processes that involve membranes such as adhesion, stacking, and fusion, especially when these processes are taking place in confined environments.

6.2 ATR-FTIR Approach

In this section we will introduce the ATR-FTIR method and present particular technical details important for understanding the results described in the chapter and subsequent discussion. Due to a relatively small light penetration depth this method is particularly suitable for conducting repeatable measurements of thin film samples under well controlled conditions.

6.2.1 ATR-FTIR Methodology

ATR-FTIR is one of the most powerful methods for recording infrared spectra of biological materials in general, and for biological membranes in particular. It yields a strong signal with only a few micrograms of sample, and allows to obtain information about the orientation of various parts of a molecule in an oriented system (Goormaghtigh et al. 1999). For example, it is possible to follow the orientation of water interacting with the polar headgroups of lipids and dependence of this orientation on temperature and lipid phase transition (Okamura et al. 1990).

(N.of E. * consider here the model discussed in Chap. 2).

The (aqueous) environment of lipid membranes can be modulated so that their properties can be studied as a function of temperature, pressure and pH, as well as in the presence of specific biologically active compounds (Tamm and Tatulian 1997; Goormaghtigh et al. 1999).

Due to the small penetration depth of IR light, the ATR-FTIR method is ideal for highly absorbing samples such as water suspensions. As the sample is brought into contact with an internal reflection element (IRE), absorption of the energy of the evanescent field by the sample provides ATR-FTIR spectra. The penetration depth d_p of IR light in the sample is defined by properties of the sample as well as the IRE and can be expressed as

$$d_p = \frac{\lambda}{\sqrt{2\pi\, n_{IRE}\left(\sin^2\theta - (n/n_{IRE})^2\right)}} \tag{6.1}$$

where λ is the wavelength of incident light, n_{IRE} is the real refractive index of the IRE, θ is the angle of incidence and n is the real refractive index of the sample. In our experiments we usually use a trapezoidal germanium plate IRE with an incidence angle of 45°. Therefore, the penetration depth d_p for hydrated lipid samples ($n \approx 1.4$) for a wavelength around the peak of the OH stretching band ($\lambda \approx 3.0$ μm) is estimated from Eq. 6.1 to be around 200 nm.

For such small d_p, almost always the low absorption approximation can be taken into account, which is applicable for reflection losses that do not exceed approximately 10 % (Harrick 1987). Even when the sample is pure water, the loss for single reflection is close to this limiting value. Within this approximation the effective thickness, i.e. the thickness of a sample that would be required to obtain the same absorption in a transmission measurement, represents proportionality constant between the reflection loss and absorption coefficient. The level of total absorbance further depends on the length of the IRE, which determines the number of active internal reflections, i.e. the number of reflections for which IR light is attenuated by a sample. In the examples that will be shown in this chapter, the number of active reflections was 13. At the used experimental conditions, the effective thickness for single reflection is about equal to the penetration depth (Harrick 1987). Therefore, the total effective sample thickness for 13 reflections is around 2.6 μm at $\lambda \approx 3.0$ μm. Due to a sufficiently low effective thickness, even bulk water can be measured under reproducible conditions and without distortion of the shape of water absorption bands. This enables detection of minute changes in the OH stretching band, which is the main objective of the presented studies.

6.2.2 Sample Preparation

The most typical way to prepare stacks of lipid membranes for ATR-FTIR measurements involves spreading of a particular volume of stock solution, e.g. chloroform

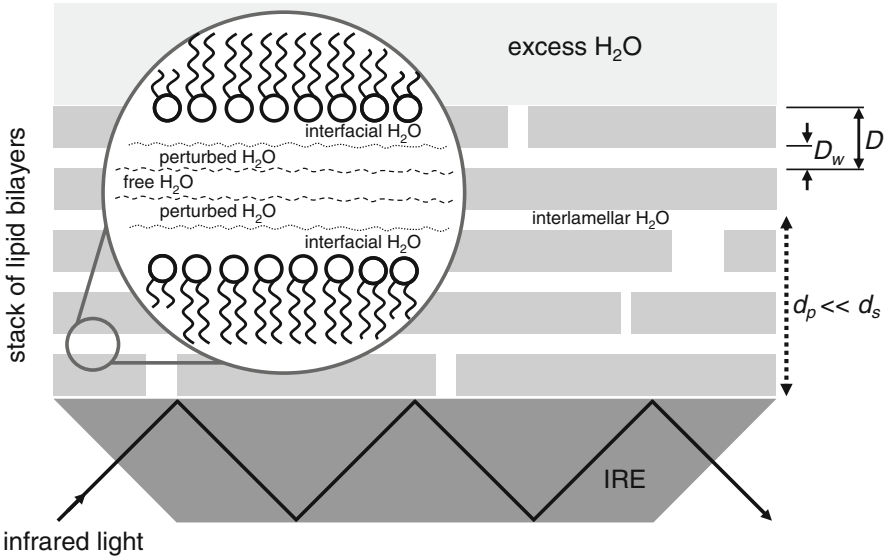

Fig. 6.1 Schematic presentation of the ATR-FTIR experimental setup. The totally reflected infrared light in the internal reflection element (IRE) is attenuated by the interaction of the sample with the evanescent field. Lipid sample in excess water is prepared to form a stack of lipid bilayers. For thick multibilayers the thickness of the stack d_s can exceed several times the penetration depth, d_p, of the evanescent field. The interlamellar water is classified as free, perturbed and interfacial water (*the zoomed inset*). The water layer thickness, D_W, and the lamellar repeat spacing, D, are also denoted. Possible defects in the lamellar structure are represented by gaps in particular bilayers

solution of lipids (Goormaghtigh et al. 1999) or water suspension of lipid vesicles (Miller and Bach 1999; Arsov and Quaroni 2007), on the properly cleaned IRE surface (Goormaghtigh et al. 1999). While the solvent is being slowly evaporated, a tip can be used to evenly spread the liquid over the surface of the IRE. This method produces a stack of highly aligned multibilayers, because capillary forces flatten the membranes during evaporation (Goormaghtigh et al. 1999). Dried lipid stacks can then be rehydrated in an atmosphere of constant relative humidity (RH) (Binder 2007) or in excess water (Arsov and Quaroni 2007).

Depending on the amount of lipids in the stock solution, thin or thick multibilayers can be formed on the IRE. In the studies that will be presented in this chapter, the thickness of the stack of lipid bilayers d_s exceeded several times the penetration depth of the evanescent wave d_p (Fig. 6.1). Figure 6.1 reveals that the water absorption in ATR-FTIR spectra for thick lipid samples, hydrated in excess water, is due to interlamellar water trapped between lipid bilayers.

It is important to note that by using multibilayers, the signal due to lipid absorption is maximized, while the signal due to water absorption is minimized. In a perfectly aligned stack without defects the water and lipid signal could be predicted from structural characteristics, such as the lamellar repeat spacing and

the water layer thickness. But for samples in excess water it usually turns out that water signal is higher and lipid signal lower than expected for the ideal lamellar sample. This is due to water present in defects (Nagle and Tristram-Nagle 2000). The defect regions, illustrated by gaps in lipid film layers in Fig. 6.1, form as a consequence of irregularities in lamellar structure and because of imperfect bilayer alignment. Nevertheless, the ratio of the water and lipid signals does not change with time significantly, showing that thick stacks of membranes are relatively stable even in excess water. It is noteworthy that the way of the lipid film preparation can affect the quality of the sample by influencing the alignment of multibilayers (Pohle et al. 1998).

Based on different attributes, such as their distance from the bilayer, H-bonding characteristics, as well as dynamic and thermodynamic properties, interlamellar water molecules are usually classified into three groups (see the zoomed inset in Fig. 6.1). (N. of E. * see Chap. 7 by Appignanessi et al.).

Different notations have been used for these groups: free water (bulk-like, far water), perturbed water (intermediate, freezable interlamellar water), and interfacial water (bound, buried, neighboring, non-freezable interlamellar water) (Kiselev et al. 1999; Kodama et al. 2001; Murzyn et al. 2006; Pinnick et al. 2010; Debnath et al. 2010). Such classification has been introduced very early also for hydration of proteins and peptides (Kuntz and Kauzmann 1974). The interfacial water is represented by water molecules that directly interact with lipids or reside in the interface region, while the free water denotes putative bulk-like molecules. The perturbed water corresponds to water in the transition region whose properties are still influenced by the presence of lipid membranes.

In order to properly interpret and understand how water properties depend on its distance from the lipid membrane and how such dependence is influenced by lipid hydration level, it is useful to know the amount and properties of water molecules belonging to particular classes. There were different attempts to quantify the number of water molecules in these different classes for example by NMR (Marinov and Dufourc 1996; Faure et al. 1997), X-ray structural studies (Nagle and Tristram-Nagle 2000) and calorimetry (Kodama et al. 2001). Useful information about the amount and properties of particular water molecules can be obtained also from molecular dynamics (MD) simulations (Pasenkiewicz-Gierula et al. 1997; Pinnick et al. 2010). However, it is difficult to define exact criteria for distinguishing different water classes.

6.2.3 Calculation of the Molar Water-to-Lipid Ratio

To relate different lipid hydration levels and the corresponding properties of interlamellar water molecules, the molar water-to-lipid ratio n_W has to be determined. It is shown in the following paragraphs how this ratio is obtained from ATR-FTIR experiments on hydrated lipid multibilayers.

In the low absorption approximation, the integral absorbance A of a vibrational mode is proportional to the concentration c of the absorbing molecules within the homogeneous film. Let us now assume that we have a layered sample. For such a heterogeneous distribution of molecules along the direction perpendicular to IRE, the contribution to absorbance at different distances from IRE should be integrated. However, in our case, where samples have a periodic structure with layers much thinner than the penetration depth, the spatial distribution of absorbing molecules within layers does not significantly influence contribution of particular layer to the absorbance. That is, for thin enough layers, the electric field amplitude can be assumed constant in each of them. Thus, the integral absorbance of water (W) or lipid (L) molecules is proportional to the corresponding effective (average) concentration across the whole sample

$$A_{W,L} \propto c_{W,L}. \tag{6.2}$$

Since the molar water-to-lipid ratio is related to the effective concentrations as

$$n_W = \frac{c_W}{c_L}, \tag{6.3}$$

it follows that n_W is proportional to the quotient of integral absorbances

$$n_W \propto \frac{A_W}{A_L}. \tag{6.4}$$

One option to determine n_W from the measured absorbance values is to find the proportionality constant in Eq. 6.4 by calibrating the absorbance quotient against n_W. Another option is presented in the proceeding paragraphs.

It was found convenient (as explained below) to use the ratio between integral absorbances of a measured sample and a reference sample, i.e. the relative integral absorbance a, for determining n_W. It is suitable to use bulk water (denoted bulk) as a reference sample for relative integral absorbance of water a_W, and dried lipid stack (denoted dry) as a reference sample for relative integral absorbance of lipids a_L. Taking into account Eq. 6.2, it then holds

$$a_W = A_W/A_W^{bulk} = c_W/c_W^{bulk} \text{ and } a_L = A_L/A_L^{dry} = c_L/c_L^{dry}, \tag{6.5}$$

where the integral absorbances are experimentally determined from spectra. It is important to note that the integral absorbance of the water OH stretching band for hydrated lipid samples should be corrected for the lipid absorption due to the overlap with lipid bands in this spectral region (and vice versa). Using Eqs. 6.3 and 6.5 the ratio n_W can be written as

$$n_W = \frac{a_W c_W^{bulk}}{a_L c_L^{dry}}. \tag{6.6}$$

The reference concentrations in Eq. 6.6 can be expressed with the corresponding molecular volumes $V^0_{W,L}$. This is useful because the values of $V^0_{W,L}$ can be evaluated from the published structural data. The general expression for the effective concentrations is

$$c_{W,L} = \frac{N_{W,L}/N_A}{V} = \frac{N_{W,L}/N_A}{N_L V^o_L + N_W V^o_W}, \tag{6.7}$$

where $N_{W,L}$ is the number of water or lipid molecules in the particular volume V, and N_A is Avogadro's number. For the bulk water reference sample the number of lipid molecules is $N_L = 0$, and for the dried lipid stack the number of water molecules is assumed to be $N_W = 0$. Therefore, it holds (as can be seen also from Eq. 6.7)

$$c^{bulk}_W = 1/N_A V^0_W,\ c^{dry}_L = 1/N_A V^0_L. \tag{6.8}$$

By considering Eqs. 6.6 and 6.8 we get

$$n_W = \frac{a_W}{a_L}\ \frac{V^0_L}{V^0_W}. \tag{6.9}$$

Using Eqs. 6.7 and 6.8 we can rewrite Eq. 6.5 as

$$a_W = \frac{N_W V^0_W}{N_L V^0_L + N_W V^0_W} \text{ and } a_L = \frac{N_L V^0_L}{N_L V^0_L + N_W V^0_W}. \tag{6.10}$$

From these two relations we can quickly realize that

$$a_W + a_L = 1. \tag{6.11}$$

Finally, Eq. 6.9 can be rewritten to obtain

$$n_W = \frac{a_W}{1 - a_W}\ \frac{V^0_L}{V^0_W}, \tag{6.12}$$

eliminating the need to measure a_L separately (but having to know the values of $V^0_{W,L}$). This explains the convenience of using the relative integral absorbances for determining n_W. Equation 6.12 was used to calculate n_W in the experimental results presented in this chapter. If the calculated n_W is related to the n_W obtained from structural data of ideal lamellar samples with the corresponding lipid composition, it is possible to estimate the level of defects in a lipid film.

To relate our derivations above to the formerly published relations between the water-to-lipid ratio and integral absorbances (Binder et al. 2001), we will also express the above equations with the swelling factor, which has been defined as

$$\phi = \frac{N_L V^0_L + N_W V^0_W}{N_L V^0_L} = 1 + n_W \frac{V^0_W}{V^0_L}. \tag{6.13}$$

By introducing Eqs. 6.9 and 6.11 in Eq. 6.13, we get

$$a_W = (\phi - 1)/\phi = n_W/\phi \frac{V_W^0}{V_L^0} \text{ and } a_L = 1/\phi\,, \tag{6.14}$$

which agrees with expressions derived previously (Binder et al. 2001)

Besides the above presented procedure, other approaches for determination of n_W according to Eq. 6.4 have been reported (Pohle et al. 1998; Miller and Bach 1999; Tielrooij et al. 2009; Gauger et al. 2010). In these studies, methyl and methylene or carbonyl lipid band absorbances are usually used to calculate lipid absorbances, while calibration is done with a method based on adding known amounts of water to a defined amount of lipids.

6.3 Structure of Water in Fully and Partially Hydrated Multibilayers

In lipid systems water content is an important variable besides temperature and composition that affects lipid phase behavior and polymorphism. Consequently, it is important to study the effect of hydration on structural and dynamical properties of lipids. This effect is reflected in different parts of IR spectrum corresponding to different lipid molecular groups such as methylene, carbonyl and phosphate groups (Grdadolnik et al. 1991; Hübner and Blume 1998; Selle and Pohle 1998; Binder 2003).

Contrary to the lipid "perspective", we can also follow a similar approach for the part of the IR spectrum, corresponding to water vibration bands. Interestingly, such studies are much less frequent. Usually, variation in the shape of the OH stretching band is followed (Grdadolnik et al. 1994; Pohle et al. 1998; Binder 2003; Disalvo et al. 2013). In the following text, we show that the shape of the OH stretching band is influenced significantly by the hydration level of multibilayers.

6.3.1 Multibilayers in Excess Water

Before we proceed to the comparison of IR spectral properties of bulk and interlamellar water, we first have to comment on the spectral behavior of pure bulk water. The shape of the OH stretching band is appreciably influenced by the temperature (Fig. 6.2). Due to the low penetration depth, ATR-FTIR is specifically suited to obtain high quality spectra of pure bulk water as explained in Sect. 6.2.1 and also highlighted previously (Maréchal 1991). Beside the drop of absorbance with higher temperature, also the shape changes significantly. As indicated by arrows in Fig. 6.2, the band peak position shifts to higher wavenumbers, the low-frequency part of the band decreases and the high-frequency part increases. This

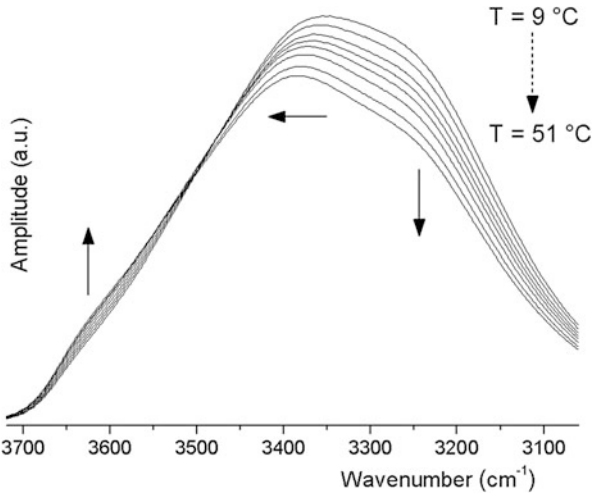

Fig. 6.2 Temperature dependence of the OH stretching band shape of pure bulk water. Spectra are shown in the interval from 9 °C to 51 °C and the temperature step is 6 °C. Beside the drop of absorbance with higher temperature also the shape changes significantly as indicated by the *solid arrows*

observation was also reported before (Brubach et al. 2005). So when we want to compare the results of the water part of IR spectrum for hydrated lipid samples at different temperatures, we have to consider also the effects of temperature on the water itself and not only the effects of lipids.

We will first present the results from multibilayers in excess water that imply the presence of interlamellar water with properties different than pure bulk water (Arsov and Quaroni 2007; Štrancar and Arsov 2008; Arsov et al. 2009). In Fig. 6.3a, the OH stretching bands for pure bulk water and interlamellar water in dimyristoylphosphatidylcholine (DMPC) multibilayers are compared. The comparison is shown for temperature above the temperature of the main phase transition for DMPC ($T_m = 24$ °C), so DMPC is observed in the liquid-crystalline or liquid-disordered phase (denoted as the Ld phase). The absorbance of water is expectedly lower in the case of the lipid sample, since beside water also lipid bilayers fill the inspected sample region.

Using Eq. 6.12 (see Sect. 6.2.3) to calculate the water-to-lipid ratio, we obtain $n_W = 52$ for the sample presented in Fig. 6.3. The values of lipid and water molecular volumes were taken from X-ray structural data (Nagle and Tristram-Nagle 2000). Let us compare this ratio to the values reported from X-ray structural data of hydrated lipid multibilayers. The values range from $n_W = 26$ for samples denoted as fully hydrated (Nagle and Tristram-Nagle 2000) to $n_W = 33$ for samples at excess water point (Costigan et al. 2000). The value calculated for our sample is significantly larger, indicating the presence of defects in our multibilayers (see Sect. 6.2.2). The value of n_W varied significantly between different samples, as it depends on the quality of the prepared multibilayers, but was always significantly higher than the n_W for ideal lamellar sample.

Despite the inferred presence of defects, it is possible to nicely discern the difference between the shape of the OH stretching band for pure bulk H_2O and

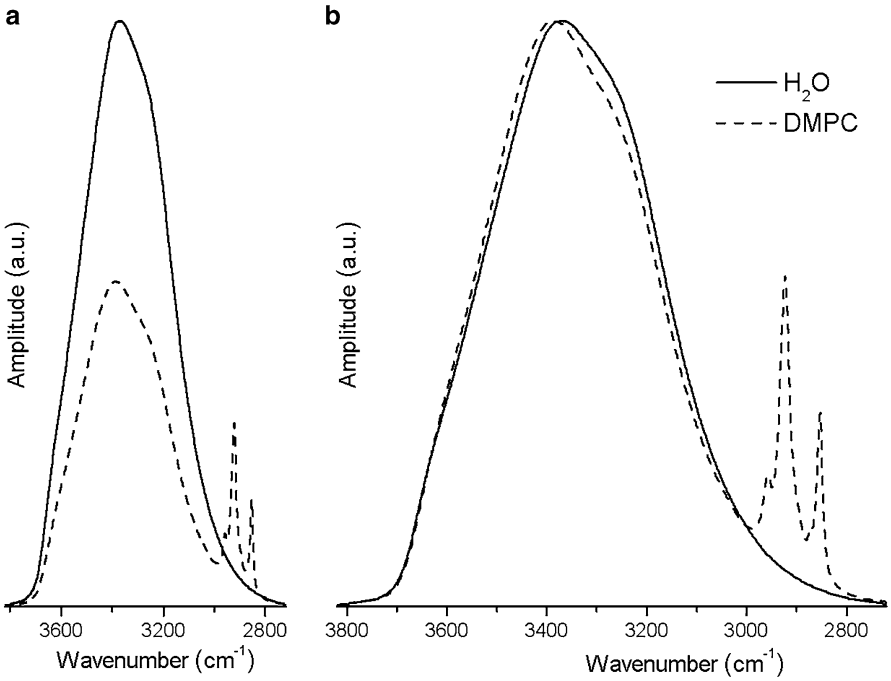

Fig. 6.3 Comparison of the OH stretching band shape for pure bulk water (H_2O) and for interlamellar water in DMPC multibilayers, prepared in excess water. Both spectra were recorded at 36 °C. (**a**) Comparison of original spectra. (**b**) Comparison of spectra after normalization to the maximum amplitude

for the interlamellar water after normalizing this part of the spectra to the maximum amplitude (Fig. 6.3b). The shift to higher frequencies could be interpreted as an overall weakening of the H-bonding among water molecules. A similar effect has been observed in the inverse micellar structures prepared from surfactants (Cringus et al. 2005), in lamellar surfactant structures (Boissière et al. 2002), and in black surfactant films (Berger et al. 2003). The observation of weakening of H-bonding is also supported by CARS data (Cheng et al. 2003; Wurpel and Müller 2006). However, for partially hydrated samples, discussed in the following section (Sect. 6.3.2), an opposite effect can be observed. This agrees with the recent statement that water properties at a weakly hydrated membrane interface are in contrast to the properties observed in inverse micelles (Volkov et al. 2007a, b).

Based on these findings, the existence of another long-range attractive contribution to the hydration force, which would compete with the fluctuation and van der Waals forces, was speculated (Arsov et al. 2009). This force should arise due to the restructuring of the interlamellar water at distances close to the equilibrium interlamellar spacing. Namely, as the water H-bonds are weakened the position of water molecules in the excess (bulk) water phase is energetically favorable,

resulting in the attractive hydration force. Attractive hydration force has indeed been proposed before. It was first suggested in the case of inter-bilayer H-bonded water bridges (Rand et al. 1988). Recently, it has been introduced to explain the observations of a DNA-dendrimer complex, where long-range interactions are facilitated by the changed local water structure (Mills et al. 2013).

In order to allow a more quantitative analysis and to enable a systematic explanation of results, the broad OH stretching band can be decomposed into a few Gaussian components (Maréchal 1991; Libnau et al. 1994; Brubach et al. 2005). Each component can be interpreted as representing water molecules with particular H-bonding properties (Brubach et al. 2005), inferring an equilibrium mixture of discrete species differing according to their specific structural arrangements. Beside the mixture models, also continuum models have been proposed, assuming that distortions of the H-bonding structure result in a continuous distribution of H-bond distances, angles, and energies (Libnau et al. 1994). Since the main aim of this chapter is only a qualitative evaluation of different effects on the structure of interlamellar water, a more in-depth analysis of the shape of the OH stretching band will be omitted. We believe this topic is worth a dedicated chapter on its own.

In addition to the strength of the H-bonds, OH stretching band shape is also influenced by the intra- and intermolecular coupling, as well as Fermi coupling of different OH vibrational modes (Sokołowska and Kęcki 1986). Since in all of the above-mentioned studies water was confined between lipid layers, the influence of the confinement or lipid-water interaction on the vibrational coupling might also cause the shape difference.

To compare the extent of the change in the strength of H-bonds with the coupling effects, experiments can be conducted in dilute solution of water (H_2O) in deuterated water (D_2O), or vice versa, where HOD molecules are dilute enough so that complete decoupling of the OH vibrational modes in HOD molecules occurs (Skinner et al. 2009). Such experiment was performed on DMPC multibilayers (Arsov et al. 2009). The corresponding OH stretching band shape difference with respect to bulk HOD exhibited a similar effect on water structure as found for samples prepared in pure H_2O. The significant upshift of the peak position confirmed that H-bonds in interlamellar water became weaker. However, the observed effect was less pronounced than in the case of pure H_2O (Arsov et al. 2009). Therefore, modifications of the vibrational coupling also play an important role in the measured OH stretching band shape, which is in line with previous findings (Lafleur et al. 1989; Sovago et al. 2008; Bonn et al. 2012).

Nevertheless, also changed coupling, especially intermolecular but also intramolecular, implies the presence of different water molecular environment (Skinner et al. 2009). Therefore, in further discussion we will not deal with exact clarification of the origin of the changed OH stretching band shape. We will simply assume that different OH stretching band shapes indicate diverse interlamellar water properties.

6.3.2 *Dehydration of Multibilayers by Water Evaporation and Osmotic Pressure*

In contrast to the samples prepared in excess water, where the OH stretching peak shifts to higher frequencies relative to the measurements on bulk water, the corresponding peak shift towards lower frequencies for partially/weakly hydrated phosphatidylcholine (PC) membranes (Grdadolnik et al. 1994; Pohle et al. 1997; Volkov et al. 2007a; Binder 2007).

These findings were reproduced also by our measurements. In order to reduce the level of hydration, the temperature was raised to a relatively high temperature (57 °C) and water slowly evaporated. This caused deswelling of multibilayers, during which the amplitude of the OH stretching band decreased, while the amplitude of lipid bands corresponding to molecular groups involving CH bonds increased (Fig. 6.4a). To compare the shape of the OH stretching band, spectra were normalized to the same maximum amplitude at the OH stretching band peak Fig. 6.4b. The comparison with the spectrum of pure bulk H_2O nicely shows that the shape for the sample in excess water ($n_W = 47$) is opposite to the dehydrated sample ($n_W = 5$). In the latter, the high-frequency side of the OH

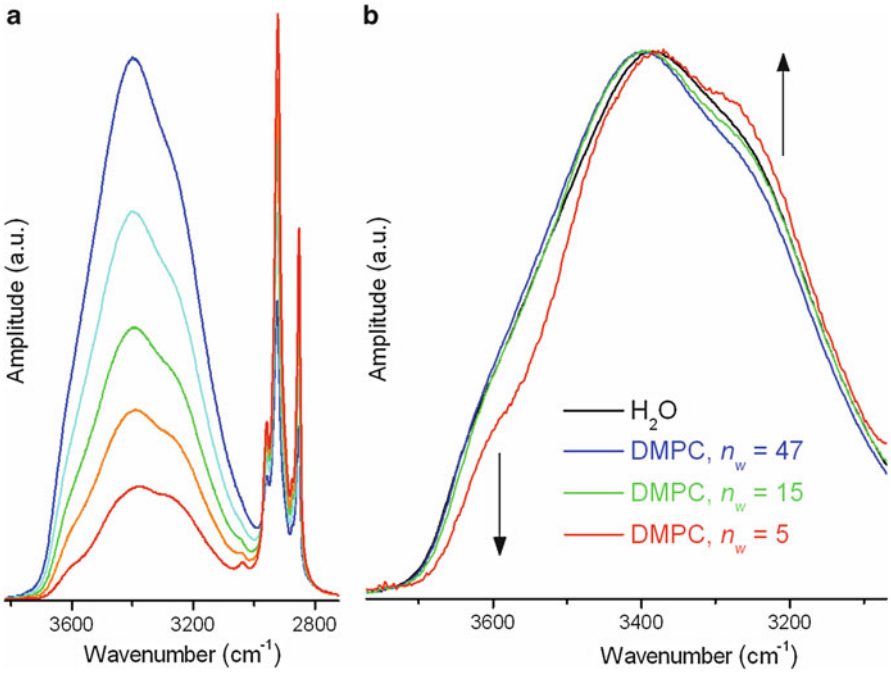

Fig. 6.4 (**a**) Deswelling of DMPC multibilayers by water evaporation (original spectra). (**b**) Comparison of the shape of the normalized OH stretching bands for pure bulk water (H_2O) and for interlamellar water in DMPC multibilayers for different n_W. *Arrows* indicate a trend in the OH stretching band shape modification upon dehydration. Spectra were recorded at 57 °C

stretching band decreases, while the low-frequency side increases relative to the spectrum of pure bulk water (as indicated by arrows in Fig. 6.4b). The level of hydration for the dehydrated sample is such that only the interfacial water remains in multibilayers (see Sect. 6.2.2 for interlamellar water classification). Therefore, the water contributing to the OH stretching band is almost entirely engaged in H-bonding directly to lipid molecular groups, e.g. phosphate and carbonyl, and not to other water molecules.

IR spectroscopy has been extensively used to characterize the hydration sites of PC showing that the primary hydration site is the phosphate group (Arrondo et al. 1984; Ter-Minassian-Saraga et al. 1988; Grdadolnik et al. 1991). Thus, the observed shift of the OH stretching band to lower frequencies is in accordance with the expected stronger hydrogen bonds between water molecules and phosphate groups relative to water-water hydrogen bonds (Bhide and Berkowitz 2005). As we will see from the results presented below (see Sect. 6.4.1), this behavior cannot be generalized to the lipids with a phosphatidylethanolamine (PE) headgroup.

It is evident that the properties of weakly hydrated lipid multibilayers significantly differ from lipid samples in excess water. The question is, how various properties are influenced for only slightly dehydrated samples. For example, lipid phase transition temperatures are not affected by water concentrations slightly below excess water point, while structural parameters such as lamellar repeat spacing are altered (Katsaras 1997; Pohle et al. 2001). As seen in Fig. 6.4b, the OH stretching band shape for DMPC already significantly changes when curves for $n_W = 47$ and $n_W = 15$ are compared, although it was reported that the thermotropic properties of DMPC are retained close to the latter value of n_W (Faure et al. 1997). Similar observations were attained by NMR measurements (Arnold et al. 1983). Thus, we have to be cautious when comparing data for samples in excess water and for the so-called "fully" hydrated samples. For example, in the experiments with IR spectroscopy where hydration level was varied through RH, the n_W values of around 12 were determined for DOPC and POPC lipids close to RH = 100 % (Pohle et al. 1998; Binder 2007). These values are much lower than expected excess water points and can probably be ascribed to the so-called vapor pressure paradox (Rand and Parsegian 1989). It was shown that the origin of this paradox is connected to a very high sensitivity of the lipid lamellar structures on small deviations of RH from 100 % (Nagle and Katsaras 1999). These deviations bring about osmotic pressure that can strongly influence the lamellar repeat spacing and consequently the value of n_W (Kucerka et al. 2005).

Another interesting conclusion can be drawn from results presented in Fig. 6.4b. Since the value $n_W = 15$ is higher than the number of interfacial water molecules per DMPC molecule of about 12 (Pasenkiewicz-Gierula et al. 1997), it can be deduced that for this sample the water removed during the evaporation came either from the population of the free water and/or from the population of the perturbed water. From the drop in the intensity of the high-frequency side of the OH stretching band, observed for DMPC as the water content was decreased from $n_W = 47$ to $n_W = 15$ (Fig. 6.4b), we can reason that the water extracted from the system cannot be classified as the bulk-like free water. Namely, if bulk-like water, whose OH

stretching band is shifted to lower frequencies with respect to the sample in excess water (Fig. 6.4b), was removed, the high-frequency side of the OH stretching band would increase. Since this is not the case, it seems that all the water removed belongs to the class of perturbed water. Consequently, we can conclude that the water structure is perturbed throughout the whole interlamellar space with thickness of about 1.8 nm in DMPC (Nagle and Tristram-Nagle 2000).

We have checked how these results compare for different dehydration procedures. We performed a similar experiment where the level of hydration was reduced by osmotic pressure through the addition of a high-molecular-weight polymer polyvinylpyrolidone (PVP). Compared to the previous dehydration procedure where higher temperature (57 °C) was required to increase the rate of water evaporation, the present procedure had no such requirements and could be conducted at lower temperature (36 °C). The addition of PVP on top of DMPC multibilayers triggered deswelling and subsequent extraction of interlamellar water as judged from the decreased OH stretching band amplitude (Fig. 6.5a). Since the thickness of the prepared multibilayers exceeds many times the penetration depth, there is no

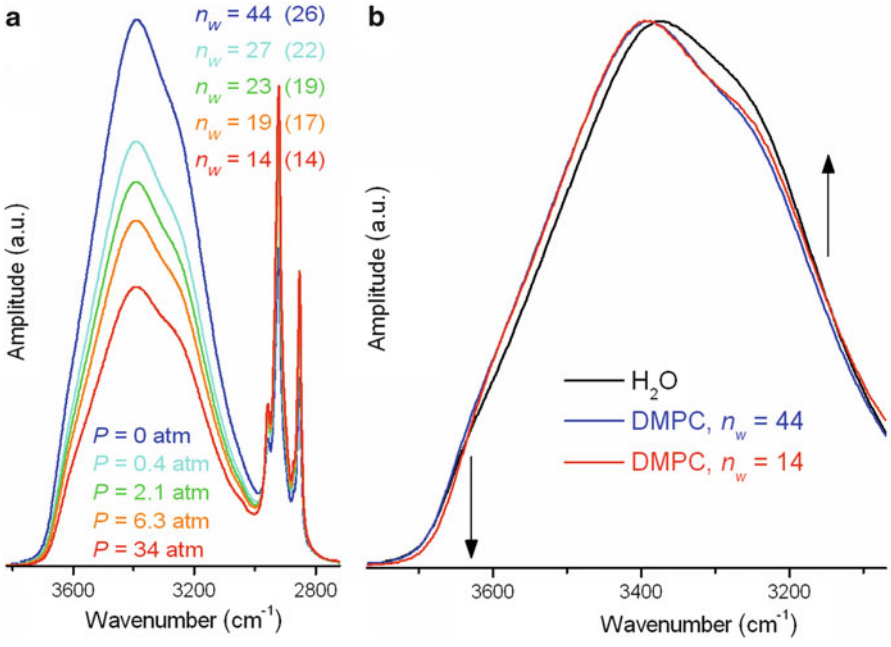

Fig. 6.5 (**a**) Deswelling of DMPC multibilayers by osmotic pressure exerted by PVP (original spectra). The marked values of osmotic pressure *P* were estimated from the weight concentration of PVP. The indicated experimentally derived values of n_W are compared to the values in *parentheses* obtained from X-ray structural studies (see text for details). (**b**) Comparison of the shape of the normalized OH stretching bands for pure bulk water (H_2O) and for interlamellar water in DMPC multibilayers for different n_W. *Arrows* indicate a trend in the OH stretching band shape modification by dehydration. Spectra were recorded at 36 °C

spectral contribution from PVP to the ATR-FTIR spectra. The values of osmotic pressure P presented in Fig. 6.5a were calculated from the amounts of added PVP. Calculation was based on interpolating function found by fitting the published data (McIntosh and Simon 1986) by a variant of functional form of dependence of osmotic pressure on PVP weight concentration (Parsegian et al. 1986).

The difference in the OH stretching band shape between DMPC in excess water ($n_W = 44$) and partially hydrated DMPC ($n_W = 14$) discerned in Fig. 6.5b was qualitatively similar to the difference observed when water was extracted by evaporation (compare to the difference between samples with $n_W = 47$ and $n_W = 15$ in Fig. 6.4b). This finding confirms that the majority of interlamellar water (beside the interfacial water) is perturbed. Similar results for the two dehydration methods are not unexpected. Recent NMR experiments indicate that the use of dehydration pressure or osmotic pressure should lead to similar effects on membrane. Namely, these two stresses are thermodynamically equivalent, since the change in chemical potential when transferring water from the interlamellar space to the bulk water phase corresponds to the induced pressure (Mallikarjunaiah et al. 2011).

The determined values of n_W for low P are higher than the values expected from X-ray structural studies (Petrache et al. 1998a, b) presented in parentheses in Fig. 6.5a. This is due to the presence of defects, i.e. irregularities in lamellar structure and imperfections in bilayer alignment. Instead of deswelling and subsequent reduction of the interlamellar repeat spacing, the osmotic pressure first reduces the number of defects, as observed before (Mennicke and Salditt 2002). Hence, only by appreciably increasing the osmotic pressure and by allowing enough time for equilibration, the values of n_W come close to the expected values (Fig. 6.5a).

Let us summarize the main conclusions drawn from Sects. 6.3.1 and 6.3.2. Firstly, we have to be careful when comparing properties of lipid bilayers in excess water and in the so-called fully hydrated samples or (even more so) in partially hydrated samples. Secondly, it seems that beside interfacial water, practically all the remaining interlamellar water can be regarded as perturbed.

6.3.3 Water Isotope and Salt Effect on the Structure of Water

The experiments presented in this chapter were conducted in pure H_2O. In contrast, to decrease the spectral overlap of particular lipid bands, e.g. carbonyl, amide or even methylene, with water bands, often D_2O is used as a solvent. Furthermore, when we want to mimic physiological conditions, membranes are usually prepared in a buffer or salt solution. It is important to be aware of the possible effects of deuterated water or salt on the structure of water.

Although the properties of liquid H_2O and D_2O are closely similar, there are small but definite differences in the magnitudes of several physical properties. For example, the degree of hydrogen bonding is higher in the case of D_2O (Némethy and Scheraga 1964). One experimental indication that D_2O has a slightly different influence on phospholipid bilayers relative to ordinary H_2O, was

offered by comparison of the carbonyl band peak position in the two solvents (Arsov and Quaroni 2007). Several computational studies confirmed these findings. One work showed that isotope substitution affects the local arrangement of the hydrogen-bonded network (Bergmann et al. 2007), while another study offered a molecular concept for this observation (Róg et al. 2009). Theoretical predictions of the latter study were also verified by fluorescence measurements on lipid membranes, where the water isotope effect on headgroup hydration and mobility, lateral lipid diffusion and lipid backbone packing was determined (Beranová et al. 2012). Substituting H_2O for D_2O can pose another problem, as H/D exchange of exchangeable sample protons can occur (Lewis and McElhaney 2007). This results in loss of the absorption band of the protonated species and its replacement with the absorption band of the deuterated species at lower frequencies. Consequently, depending on the band concerned, spectroscopic observation may not be convenient.

The knowledge of the ion-specific hydration effect at the interface between the phospholipid bilayer and aqueous solution has greatly improved lately. But despite substantial progress, many issues remain unresolved (Parsegian and Zemb 2011). Diverse efforts have been undertaken in this respect. It was studied by ATR-FTIR how different aqueous solutions of salts at diverse concentrations modify the OH stretching band (Riemenschneider et al. 2008). The effect on the structure of water upon addition of salts was examined also by Raman spectroscopy (Cavaille et al. 1996). Furthermore, a surface-sensitive vibrational sum frequency generation method was used to examine how the water structure at the lipid-water interface is affected by the presence of ions (Chen et al. 2010). Structural properties of pure water and ionic solutions were also compared through measurement of the orientational-correlation time of water molecules by femtosecond pump–probe spectroscopy (Omta et al. 2003). Moreover, it has been suggested recently that the swelling of neutral lipid bilayers upon addition of a salt cannot be explained only by the screening of the van der Waals interactions, but that also increase in the hydration force has to be taken into account (Manciu and Ruckenstein 2007).

6.4 Influence of Lipid Composition/Phase on the Structure of Interlamellar Water

Lipid composition and lipid phase of multibilayers influence the excess water point and structural characteristics such as lamellar repeat spacing and interlamellar water layer thickness. Consequently, the force balance between bilayers changes with temperature and lipid composition of membranes. Therefore, it can be anticipated that also interlamellar water properties as well as the corresponding hydration force contribution might be modified by these characteristics, as will be outlined throughout this section.

6.4.1 *Influence of Lipid Composition*

In order to study the influence of lipid composition and to compare the results to those obtained on DMPC multibilayers, shown above, measurements with samples prepared from palmitoyloleoylphosphatidylethanolamine (POPE) were conducted. This lipid was chosen because it differs with regards to DMPC in its headgroup, affecting the interfacial water, and because it has much smaller interlamellar repeat spacing, implying a different balance of forces between bilayers (McIntosh and Simon 1996).

From the inset to Fig. 6.6a, we can nicely appreciate that the amplitude of DMPC spectrum is higher than that of POPE spectrum in the OH stretching band region. This observation is expected, since the lamellar repeat spacing is much smaller in the case of POPE, which explains much smaller water-to-lipid ratio n_W. In order to better compare the OH stretching band shapes, Fig. 6.6a shows the normalized spectra against the corresponding spectrum of pure bulk H_2O. Similar observations follow for POPE as mentioned previously in the case of DMPC. The increase in the high-frequency part is even more pronounced than for DMPC, while the low-

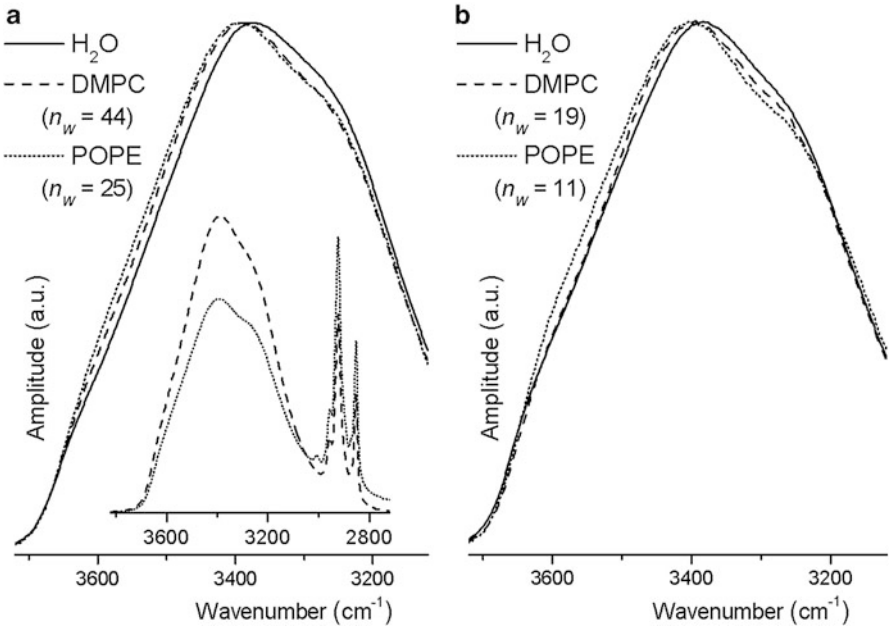

Fig. 6.6 Comparison of the OH stretching band shape for pure bulk water (H_2O) and for interlamellar water in DMPC and POPE multibilayers. (**a**) Comparison before (*inset*) and after normalization to the maximum amplitude (main plot) for samples in excess water. Spectra were recorded at 36 °C. (**b**) Comparison with normalization to the maximum amplitude for partially dehydrated samples. Spectra were recorded at 57 °C. Two representative spectra are compared to the spectrum for pure bulk water

frequency part of the spectra seems comparable. There are two possible explanations for this difference. Either the average H-bonding is even more weakened than in DMPC and/or higher confinement of water in the case of POPE more strongly influences the coupling of water vibrational modes (see Sect. 6.3.1). In the case of POPE, there is no free water present between bilayers because of a very small interlamellar repeat spacing of around 0.6 nm (Rappolt et al. 2003). So, interlamellar water is represented only by the interfacial and the perturbed water. Therefore, the increase in the intensity of the high-frequency side of the OH stretching band for POPE with respect to pure bulk H_2O is due to the structure of the perturbed water (Fig. 6.6).

Similar to DMPC, the determined value of $n_W = 25$ for POPE in excess water (Fig. 6.6a) is larger than expected from structural or NMR data that yield n_W of around 15 (Marinov and Dufourc 1996; Rappolt et al. 2003). Thus, also our POPE multibilayers contain defects and are irregular to some extent. In order to exclude a possibility that the difference in the spectral shapes between DMPC and POPE arose mainly because of a relatively larger amount of interlamellar water due to the defects for DMPC, the comparison between samples partially dehydrated by water evaporation was done (Fig. 6.6b). The value of n_W in this case is below the fully hydrated level but above the level where only the interfacial water is present, which is around $n_W = 12$ for DMPC (Pasenkiewicz-Gierula et al. 1997) and around $n_W = 8$ for POPE (Marinov and Dufourc 1996), respectively. As we saw above in the experiment with osmotic pressure, we can expect that the dehydration reduces the number of defects in the lamellar structure. The difference between DMPC and POPE remains qualitatively the same (compare Fig. 6.6a, b), which suggests that it originates from particular lipid-water interaction properties and not from the difference in the quality of sample preparation.

Further spectra of POPE multibilayers before and after sequential dehydration by water evaporation are presented in Fig. 6.7. Deswelling of POPE multibilayers is nicely discerned (Fig. 6.7a). Next, the OH stretching band shape was compared for different n_W. The situation for partially hydrated POPE samples (Fig. 6.7b) is markedly different from what is seen in DMPC (Fig. 6.4b). Here even when only interfacial water molecules remain in the system ($n_W = 5$, Fig. 6.7b), the shape of the OH stretching band and the peak position do not significantly differ from the sample in excess water ($n_W = 23$, Fig. 6.7b). This observation is especially trustful for frequencies above 3400 cm^{-1}. At lower frequencies, between roughly 3400 cm^{-1} and 3000 cm^{-1}, the POPE absorption due to the stretching vibrations of ethanolamine group (Fringeli and Günthard 1981) shown in Fig. 6.8a, disturbs the comparison. In order to diminish this disturbance, properly weighted spectrum of dry POPE was subtracted from the original spectra (Fig. 6.7b).

As seen in Fig. 6.7b, the OH stretching band for weakly hydrated POPE is not shifted to lower frequencies with respect to pure bulk H_2O, Therefore, the corresponding shift observed for partially hydrated PC membranes, is strongly correlated to the properties of the PC headgroup and not to some intrinsic lipid bilayer effect on the water structure. This specific interaction is also reflected in the fact that it is possible to remove almost all the bound water from PE membranes by

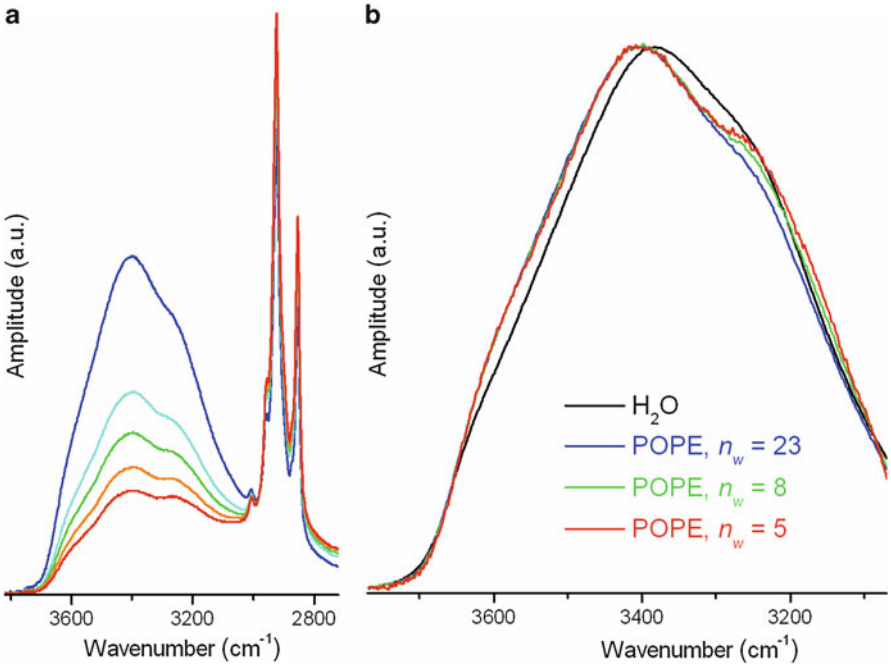

Fig. 6.7 (**a**) Deswelling of POPE multibilayers by water evaporation (original spectra). (**b**) Comparison of the shape of the normalized OH stretching bands for pure bulk water (H_2O) and for interlamellar water in POPE multibilayers for different n_W. Properly weighted spectrum of dry POPE was subtracted from the original spectra to reduce the contribution of lipid absorption in the inspected spectral range (for details see text). Spectra were recorded at 57 °C

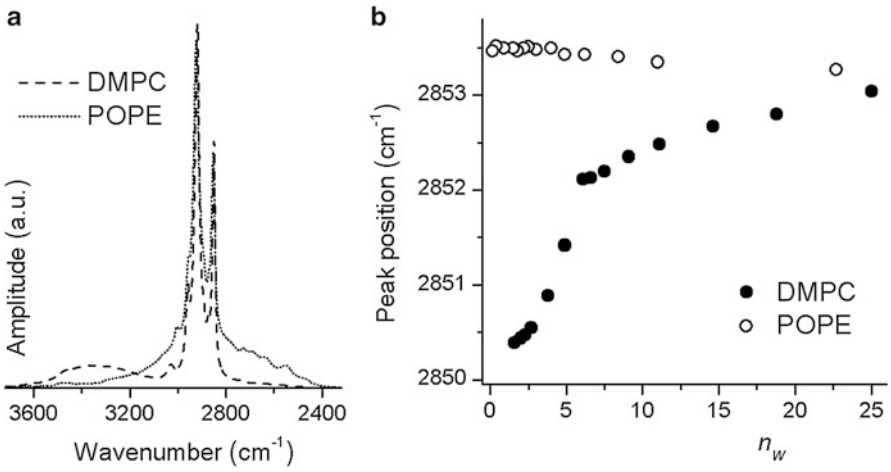

Fig. 6.8 (**a**) Comparison of spectra for DMPC and POPE multibilayers gently dried by evaporation and recorded at 57 °C. (**b**) Dependence of the symmetric methylene (CH_2) stretching band peak position on the molar water-to-lipid ratio n_W

drying the stack of lipid bilayers under gentle conditions (Pohle and Selle 1996). In contrast, some interfacial water, presumably tightly bound to phosphate groups and represented by a broad absorption band from approximately 3700 cm^{-1} to 3100 cm^{-1}, remains trapped in the case of PC (Fig. 6.8a).

Moreover, dependence of lipid phases on the water content in the system, i.e. lyotropic properties, changes as well. As can be seen from Fig. 6.8b, the lyotropic main phase transition of lipids can be detected from dependence of symmetric methylene (CH_2) stretching band peak position on hydration level of DMPC as expected from the literature (Markova et al. 2000; Binder 2003). This transition is absent for POPE, in accordance with previously published results for PE lipids (Selle et al. 1999; Binder 2003).

There are other evidences for the difference between properties of water amongst layers of PC and PE membranes. For example, significant variations exist in the portions of water molecules belonging to different classes of interlamellar water as determined by calorimetric approaches (Kodama et al. 1997, 2001). Furthermore, an FTIR study revealed that the intermolecular H-bonding interaction between amine and phosphate groups in POPE considerably modifies the hydration properties of PE lipids (Bouchet et al. 2009). In addition, computational studies showed that the ethanolamine group of PE affects water structure and motion differently than the equivalent choline group of PC (Damodaran and Merz 1993; Murzyn et al. 2006).

From the discussion above it follows that the lipid composition can affect interlamellar water structure not only in the interfacial water population but also farther away from the membrane. Therefore, the long-range lipid-water interaction could be modulated by the lipid composition.

6.4.2 Influence of Lipid Phase

Lipids in excess water can exist in different phases depending on the temperature. For example, at low temperatures phosphatidylcholine membranes are found in the gel or solid-ordered phase (S phase), just below the main phase transition temperature in the ripple phase, and above this temperature in the liquid-crystalline or liquid-disordered phase (Ld phase) (Janiak et al. 1979). High concentrations of added cholesterol (Chol) can lead to the liquid-ordered phase (Lo phase) (Ipsen et al. 1987). Similar phase behavior is observed also for phosphatidylethanolamines, but additionally the so-called inverted hexagonal phase (H_{II} phase) appears at higher temperatures (Mantsch 1984; Paré and Lafleur 1998).

IR spectroscopy has long been a valuable tool for studying phase transitions as well as the properties of different lipid phases. In this respect, it is especially worthwhile to follow the lipid part of an IR spectrum, i.e. the temperature dependence of the peak position of the methylene (CH_2) stretching bands or of the carbonyl ($C=O$) stretching band (Casal and Mantsch 1984; Mantsch and McElhaney 1991; Lewis and McElhaney 2007; Arsov and Quaroni 2007). Because of the interaction

between lipid and water molecules, it would be interesting to examine whether lipid thermotropic characteristics are reflected also in the water part of IR spectrum.

Recently, there have been several attempts to check the influence of different lipid phases on the OH stretching band shape in samples prepared in excess water. It was reported that the difference between the S phase and the Ld phase can be appreciated for DMPC by correlating the temperature behavior of the carbonyl band with the evolution of the OH stretching band shape (Disalvo and Frias 2013). This finding is supported by MD simulations, which have shown that local hydration of carbonyl groups differ between the S and the Ld phase (Stepniewski et al. 2010).

We have shown that the difference in the water part of IR spectrum, although relatively small, can be appreciated also when we compare the S phase and the Lo phase for DMPC and DMPC samples containing 40 mol% of cholesterol (DMPC/Chol 0.4), respectively (Štrancar and Arsov 2008). We analyzed for possible changes also samples above the temperature of the main phase transition, but we observed no significant differences between samples in the Ld and the Lo phase. We know from structural measurements that the interlamellar water layer thickness decreases and bilayer thickness increases with higher concentration of cholesterol (Hodzic et al. 2008; Gallová et al. 2011). This could have two possible implications. The straightforward one is that the amplitude of the OH stretching band should decrease in the samples with cholesterol. Unfortunately, in our excess water experiments this amplitude depends significantly on the quality of the sample preparation, i.e. on the number and size of defects in multibilayers. It therefore seems that adding cholesterol enhances formation of defects. The second effect could be an alteration in the shape of the OH stretching band. Since an influence of the Lo phase was not detected, as noted above, it is possible that the influence is reflected mainly in the population of interfacial water. Consequently, due to a relatively small contribution of interfacial water to the overall water signal, the expected difference between DMPC and DMPC/Chol multibilayers might be obscured.

Similar to the expectation for the Ld and the Lo phase, an abrupt change in the structural parameters at the main phase transition between the S and the Ld phase is anticipated to affect the amplitude of the OH stretching band. In this case, contrary to the Ld/Lo comparison, the change in the amplitude is nicely discerned around the temperature of the main S-to-Ld phase transition in DMPC (Fig. 6.9a). Even though the spectra are taken at temperatures that are apart for 3 °C, this difference is large enough not to be a consequence of the intrinsic pure bulk water OH stretching band temperature dependence (Fig. 6.2). However, the observed decrease in the amplitude is opposite to what we would expect from structural data, which show that the amount of interlamellar water increases from the S phase (Tristram-Nagle et al. 2002) to the Ld phase (Kucerka et al. 2005). Possibly, the effect of additional swelling in the Ld phase competes with reduction of the number of defects due to the presence of a more adaptable liquid lipid phase.

The altered amplitude of the OH stretching band can be appreciated also at the Ld-to-H_{II} phase transition for POPE/Chol 0.2 multibilayers in excess water (Fig. 6.9b). Here the change is much more dramatic. The temperature of the amplitude jump coincides with the expected temperature for the Ld-to-H_{II} phase

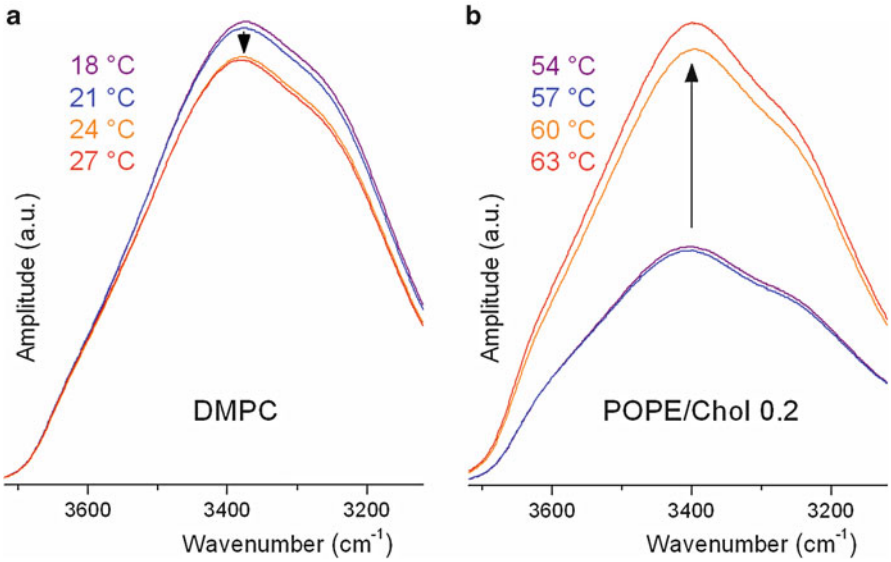

Fig. 6.9 Evolution of the shape of the OH stretching band for interlamellar water around the phase transition temperature in (**a**) DMPC and (**b**) POPE/Chol 0.2 multibilayers prepared in excess water. The temperature at which particular spectrum was recorded is indicated. In the case of DMPC, the S-to-Ld phase transition is discerned from the sudden change in the OH stretching band amplitude as denoted by the *arrow*. Similarly, for POPE/Chol 0.2 the Ld-to-H_{II} phase transition is detected

transition of around 55 °C (Paré and Lafleur 1998). The amplitude rise also agrees with the expected increase of n_W from the Ld phase to the H_{II} phase (Rand and Fuller 1994; Marinov and Dufourc 1996). However, the change is much larger than expected from this increase. It seems that in this case the phase transition triggers the formation of defects in lipid samples.

We have additionally confirmed that this really represents the Ld-to-H_{II} phase transition by measuring the temperature dependence of the peak position of the methylene symmetric stretching band for POPE and POPE/Chol 0.2 samples (Fig. 6.10a). Our measurements nicely reproduce previously published results (Paré and Lafleur 1998). The arrow in Fig. 6.10a also demonstrates that the temperature at which the jump in the peak position of the methylene symmetric stretching band for POPE/Chol 0.2 sample occurs matches the temperature at which the jump in the OH stretching band amplitude is seen (Fig. 6.9b).

To finally check the effect of the phase transition on the structure of interlamellar water, we also compared the OH stretching band shape for POPE/Chol 0.2 sample just below and above the Ld-to-H_{II} phase transition (Fig. 6.10b). As we saw in Fig. 6.9b, the lamellar structure strongly swells on account of defects that arise at the Ld-to-H_{II} phase transition. However, from the discussion in Sect. 6.4.1 and from the results presented in Fig. 6.6, where we showed that the spectral changes between DMPC and POPE did not arise from a relatively larger amount of interlamellar

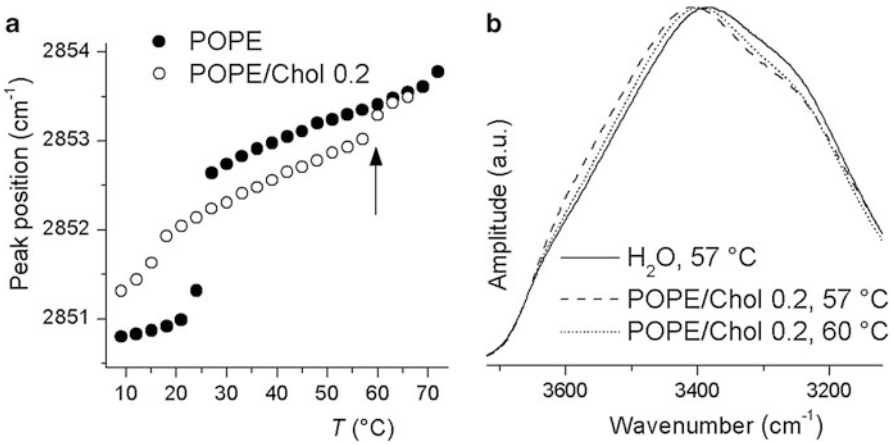

Fig. 6.10 (**a**) Temperature dependence of the symmetric methylene (CH_2) stretching band peak position for POPE and POPE/Chol 0.2. The main phase transition for POPE at around 25 °C and the Ld-to-H_{II} phase transition for POPE/Chol 0.2 (indicated by *arrow*) can nicely be recognized. (**b**) Comparison of the shape of the OH stretching band for interlamellar water in POPE/Chol 0.2 multibilayers prepared in excess water for temperature below and above the Ld-to-H_{II} phase transition. The temperature at which each particular spectrum was recorded is indicated

water due to the defects for DMPC, it seems reasonable to conclude that the OH stretching band shape in the case of POPE/Chol 0.2 changes because of the lipid phase transition and not because of the reduced quality of the sample. Therefore, in this case the influence of the lipid phase is reflected also in the interlamellar water structure.

6.5 The Long-Range Lipid-Water Interaction

Experimental evidence presented in the previous sections points to the presence of a long-range lipid-water interaction in lipid multibilayers. As emphasized above, by "long-range" it is meant that a large part or even all interlamellar water, beside interfacial water, can be classified as perturbed. Hence, contrary to the more general view, there seem to be more than one or two hydration water layers perturbed. Taking into account the typical dimension of a water molecule of around 0.3 nm, and the typical interlamellar water layer thickness in PC multibilayers of around 1.8 nm, there could be roughly three hydration layers on each side of a PC lipid bilayer expanding about 0.9 nm from the bilayer surface. Therefore, each water property in this range of distance from bilayer surface that is different from bulk water indicates a long-range effect.

Results of other experimental methods also offer support of the long-range lipid-water interaction, as discussed further in this section. This finding could influence

the understanding of water-mediated processes in confined regions between membranes. Nevertheless, it is still questionable whether this long-range interaction is strong enough to influence any physical or chemical process and how this strength is modified by different lipid composition or lipid phase. However, a small perturbation of many molecules can add up to significant forces, strong enough to deform the force balance. For example, moving two bilayers together by the size of a water molecule amounts to a displacement of a large number of water molecules due to relatively large surface area of the bilayers, requiring significant work input (Parsegian and Zemb 2011).

6.5.1 The Long-Range Interaction as Observed by Different Methods

It was observed quite early by MD simulations that the water density profile along the normal to the membrane changes much farther away than for one water hydration layer (Pandit et al. 2003; Berkowitz et al. 2006; Debnath et al. 2010). In another MD study it was noticed that some properties do not change beyond the commonly established excess water point, but water diffusion coefficient still increases upon further hydration (Pinnick et al. 2010). Similarly, it was shown that diffusion rates settle to their bulk water values only as far as 1.0 nm away from the lipid surface (Hansen et al. 2012), what can be regarded as a long-range effect based on the criteria mentioned in the introduction to this section. Another example revealed that orientational relaxation of hydration water is still slower than in the bulk water, although the hydration level was above the full hydration level of the studied bilayer (Zhang and Berkowitz 2009).

As can be seen from the discussion above, both structural and dynamical properties of water can be influenced far away, i.e. around 1.0 nm, from the water-membrane interface. Therefore, we can conclude that when two opposing bilayers come close, almost none of the molecules will have bulk-like water properties.

Not only computational but also experimental techniques confirm the notion of the long-range lipid-water interaction. Here structural and dynamical properties can be characterized. It has to be noted, with regard to the experimental emphasis of this chapter, that ATR-FTIR does not offer information on the dynamics of water molecules. It has been shown that substantial differences in dynamics can exist between samples, even when IR absorption spectra are similar. By augmenting conventional spectra with time-resolved studies, e.g. IR pump-probe spectroscopy, ambiguous interpretations of the relative structure and dynamical behavior of water in different environments can be avoided (Piletic et al. 2006).

Work with frequency modulation atomic force microscopy (AFM) revealed an oscillatory hydration force with distance from the lipid surface, which suggested that water is organized in at least two or more structured hydration layers (Higgins et al. 2006; Fukuma et al. 2007). Interestingly, the force profile is influenced by the lipid phase (Higgins et al. 2006).

Fluorescence time-resolved measurements showed that three hydration water layers, including the interfacial water, are perturbed in a confined environment. These findings were based on measuring relaxation dynamics profile of confined water in aqueous nanochannels of the lipidic cubic phase mapped out with femtosecond resolution across the nanochannel (Kim et al. 2006).

(* N. of E. for details in fluorescent methodologies and interfacial water see Chap. 5)

The hydration state of phospholipid bilayers can also be precisely studied by terahertz spectroscopy. By this method, water perturbed by a lipid membrane is detected from the observation of the relaxation dynamics of water molecules in the subpicosecond time scale. Combined with X-ray observation of the lamellar structure of the lipids, a long-range hydration effect on up to four to five layers of water was confirmed (Hishida and Tanaka 2011).

Although no unique picture exists, there are many different indications about the perturbation of water properties beyond the so-called interfacial water or the first hydration water layer. This supports the view that in confined membrane environments water structure can be different than in bulk. This might have an important impact on water-mediated biological processes. (* N. of E. Further discussion on this topic can be found in Chap. 7)

6.5.2 Possible Implications of the Long-Range Interaction in Confined Environments

Coupling phenomena between membranes, such as adhesion, stacking, and fusion, could be influenced by water-mediated effects. Experimental results also demonstrate that hydration layers are stable enough to present energy barriers to approaching nanoscale objects, such as proteins and solvated ions, and are therefore expected to affect membrane permeability and transport (Fukuma et al. 2007). Therefore, an important open question is how exactly the water structure is affected by a nanometer-scale confinement (Levinger 2002), because water confined to narrow spaces may no longer resemble that in the bulk (Guo et al. 2005). This holds true for lipid model systems as well as for cellular environments. For example, organelle-specific water structure was resolved with Raman microspectroscopy (Tiwari et al. 2013). Similarly to membrane-based processes, water is expected to have an essential role also in adapting protein conformational properties in confined environments. In the following, some examples of implication of long-range lipid-water interaction will be presented.

First example is the phase-governed stacking of lipid domains in phase-separated multibilayers. It was speculated that differences in water networks for the Lo and Ld phases could produce distinct lipid-water interfaces for the coexisting lipid domains. The mismatch of the water network introduces an energetically unfavorable penalty at the interface where the two networks join. Lipid domain alignment across the

lipid layers reduces such interfaces and thus lowers the overall free energy of the system, suggesting a plausible mechanism for the observed interlamellar domain ordering (Tayebi et al. 2012). The mentioned assumptions are supported by our as well as several other independent observations of lipid phase influence on hydration water properties. Ultrahigh resolution frequency modulation AFM imaging suggested possible different hydration structures around particular membrane raft-like domains that could present significant energy barriers to interacting biomolecules (Sheikh and Jarvis 2011). Although raft hydration layers would not exclude other membrane-associated proteins or external biomolecules from interacting with raft-associated proteins, they could modulate the spatial location and kinetics of these interactions.

Another example of a possible water structure-mediated interaction was brought by a computational study of vesicle fusion. In this survey, results show not only that the dynamics of water between two membranes is altered, but also that the conformational state of this water can control the fusion reaction between the two membranes. In this case, water helps the vesicles stick to each other by slowing lipid rearrangements at the interface that are necessary for fusion (Kasson et al. 2011).

Analogous to lipid bilayers, aqueous solvent and hydrophobic interaction play also a major role for the polypeptide chain folding in globular proteins and for the conformational stability and flexibility of proteins. Specifically for proteins, the dynamics of water–protein interactions govern various activities, including the facilitation of protein folding, maintenance of structural integrity, mediation of molecular recognition, and acceleration of enzymatic catalysis (Zhong et al. 2011). The coupling between dynamics of water structure and protein dynamics is considered to play an important role in protein folding. The experimental data obtained by terahertz spectroscopy suggests a long-range influence on the correlated motion of water molecules in the protein hydration water network (Ebbinghaus et al. 2007). It was also shown by MD simulation that confining both protein and solvent gives rise to a solvent-mediated effect that destabilizes the native structure of the protein. Thus, it was demonstrated that the confinement of solvent has a significant impact on protein kinetics and thermodynamics (Lucent et al. 2007). MD simulations were also used to explore the effects of unfolding on the dynamical behavior of water present in the hydration layers of different segments of the protein (Chakraborty and Bandyopadhyay 2008).

6.6 Concluding Remarks

The application of ATR-FTIR to study the properties of interlamellar water in lipid multibilayers, prepared in excess water, enabled us to show the presence of the long-range lipid-water interaction. In addition, there are many indications that lipid composition and phase properties modify this interaction. Consequently, it is likely that biological processes taking place in confined environments between membranes are influenced by this long-range interaction at appreciable distances, even before

the membranes are in direct contact. This can have important implications for understanding the role of water in membrane-mediated processes. Further studies are needed to precisely elucidate the unique significance of structural and dynamical properties of water for different processes. The interest in further research in this area is rapidly growing and will in the future undoubtedly fit water into the wider picture of its biological relevance.

Acknowledgments The financial support from the state budget by the Slovenian Research Agency (program No. P1-0060) is acknowledged. The author appreciates collaboration or helpful discussions with Luca Quaroni, Michael Rappolt, Joze Grdadolnik, Primoz Ziherl and Rudolf Podgornik. The author also thanks Iztok Urbancic for carefully reading this manuscript.

References

Arnold K, Pratsch L, Gawrisch K (1983) Effect of poly(ethylene glycol) on phospholipid hydration and polarity of the external phase. Biochim Biophys Acta 728:121–128

Arrondo J, Goni F, Macarulla J (1984) Infrared spectroscopy of phosphatidylcholines in aqueous suspension a study of the phosphate group vibrations. Biochim Biophys Acta 794:165–168

Arsov Z, Quaroni L (2007) Direct interaction between cholesterol and phosphatidylcholines in hydrated membranes revealed by ATR-FTIR spectroscopy. Chem Phys Lipids 150:35–48

Arsov Z, Rappolt M, Grdadolnik J (2009) Weakened hydrogen bonds in water confined between lipid bilayers: the existence of a long-range attractive hydration force. Chemphyschem 10:1438–1441

Ball P (2008a) Water as a biomolecule. Chemphyschem 9:2677–2685

Ball P (2008b) Water as an active constituent in cell biology. Chem Rev 108:74–108

Beranová L, Humpolíčková J, Sýkora J et al (2012) Effect of heavy water on phospholipid membranes: experimental confirmation of molecular dynamics simulations. Phys Chem Chem Phys 14:14516–14522

Berger C, Desbat B, Kellay H et al (2003) Water confinement effects in black soap films. Langmuir 19:1–5

Bergmann U, Nordlund D, Wernet P et al (2007) Isotope effects in liquid water probed by x-ray Raman spectroscopy. Phys Rev B 76:024202

Berkowitz ML, Vácha R (2012) Aqueous solutions at the interface with phospholipid bilayers. Acc Chem Res 45:74–82

Berkowitz ML, Bostick DL, Pandit S (2006) Aqueous solutions next to phospholipid membrane surfaces: insights from simulations. Chem Rev 106:1527–1539

Bhide SY, Berkowitz ML (2005) Structure and dynamics of water at the interface with phospholipid bilayers. J Chem Phys 123:224702

Binder H (2003) The molecular architecture of lipid membranes—new insights from hydration-tuning infrared linear dichroism spectroscopy. Appl Spectrosc Rev 38:15–69

Binder H (2007) Water near lipid membranes as seen by infrared spectroscopy. Eur Biophys J 36:265–279

Binder H, Arnold K, Ulrich AS, Zschörnig O (2001) Interaction of Zn2+ with phospholipid membranes. Biophys Chem 90:57–74

Boissière C, Brubach JB, Mermet A et al (2002) Water confined in lamellar structures of AOT surfactants: an infrared investigation. J Phys Chem B 106:1032–1035

Bonn M, Bakker HJ, Tong Y, Backus EHG (2012) No ice-like water at aqueous biological interfaces. Biointerphases 7:20

Bouchet AM, Frías MA, Lairion F et al (2009) Structural and dynamical surface properties of phosphatidylethanolamine containing membranes. Biochim Biophys Acta 1788:918–925
Brubach J-B, Mermet A, Filabozzi A et al (2005) Signatures of the hydrogen bonding in the infrared bands of water. J Chem Phys 122:184509
Casal H, Mantsch H (1984) Polymorphic phase behaviour of phospholipid membranes studied by infrared spectroscopy. Biochim Biophys Acta Rev Biomembr 779:381–401
Cavaille D, Combes D, Zwick A (1996) Effect of high hydrostatic pressure and additives on the dynamics of water: a Raman spectroscopy study. J Raman Spectrosc 27:853–857
Chakraborty S, Bandyopadhyay S (2008) Dynamics of water in the hydration layer of a partially unfolded structure of the protein HP-36. J Phys Chem B 112:6500–6507
Chaplin M (2006) Do we underestimate the importance of water in cell biology? Nat Rev Mol Cell Biol 7:861–866
Chen X, Hua W, Huang Z, Allen HC (2010) Interfacial water structure associated with phospholipid membranes studied by phase-sensitive vibrational sum frequency generation spectroscopy. J Am Chem Soc 132:11336–11342
Cheng J-X, Pautot S, Weitz DA, Xie XS (2003) Ordering of water molecules between phospholipid bilayers visualized by coherent anti-Stokes Raman scattering microscopy. Proc Natl Acad Sci U S A 100:9826–9830
Costigan SC, Booth PJ, Templer RH (2000) Estimations of lipid bilayer geometry in fluid lamellar phases. Biochim Biophys Acta 1468:41–54
Cringus D, Lindner J, Milder MTW et al (2005) Femtosecond water dynamics in reverse-micellar nanodroplets. Chem Phys Lett 408:162–168
Damodaran K, Merz K (1993) Head group-water interactions in lipid bilayers: a comparison between DMPC-and DLPE-based lipid bilayers. Langmuir 9:1179–1183
Debnath A, Mukherjee B, Ayappa KG et al (2010) Entropy and dynamics of water in hydration layers of a bilayer. J Chem Phys 133:174704
Disalvo EA, Frias MA (2013) Water state and carbonyl distribution populations in confined regions of lipid bilayers observed by FTIR spectroscopy. Langmuir 29:6969–6974
Disalvo EA, Lairion F, Martini F et al (2008) Structural and functional properties of hydration and confined water in membrane interfaces. Biochim Biophys Acta 1778:2655–2670
Disalvo EA, Bouchet AM, Frias MA (2013) Connected and isolated CH2 populations in acyl chains and its relation to pockets of confined water in lipid membranes as observed by FTIR spectrometry. Biochim Biophys Acta 1828:1683–1689
Ebbinghaus S, Kim SJ, Heyden M et al (2007) An extended dynamical hydration shell around proteins. Proc Natl Acad Sci U S A 104:20749–20752
Faure C, Bonakdar L, Dufourc EJ (1997) Determination of DMPC hydration in the Lα and Lβ′ phases by ^{2}H solid state NMR of D2O. FEBS Lett 405:263–266
Finer E, Darke A (1974) Phospholipid hydration studied by deuteron magnetic resonance spectroscopy. Chem Phys Lipids 12:1–16
Fitter J, Lechner RE, Dencher NA (1999) Interactions of hydration water and biological membranes studied by neutron scattering. J Phys Chem B 103:8036–8050
Fringeli UP, Günthard HH (1981) Infrared membrane spectroscopy. In: Grell E (ed) Membrane spectroscopy. Springer, Berlin, pp 270–332
Fukuma T, Higgins MJ, Jarvis SP (2007) Direct imaging of individual intrinsic hydration layers on lipid bilayers at Angstrom resolution. Biophys J 92:3603–3609
Gallová J, Uhríková D, Kučerka N et al (2011) The effects of cholesterol and β-sitosterol on the structure of saturated diacylphosphatidylcholine bilayers. Eur Biophys J 40:153–163
Gauger DR, Andrushchenko VV, Bour P, Pohle W (2010) A spectroscopic method to estimate the binding potency of amphiphile assemblies. Anal Bioanal Chem 398:1109–1123
Goormaghtigh E, Raussens V, Ruysschaert JM (1999) Attenuated total reflection infrared spectroscopy of proteins and lipids in biological membranes. Biochim Biophys Acta 1422:105–185
Grdadolnik J, Kidrič J, Hadži D (1991) Hydration of phosphatidylcholine reverse micelles and multilayers—an infrared spectroscopic study. Chem Phys Lipids 59:57–68

Grdadolnik J, Kidrič J, Hadži D (1994) An FT-IR study of water hydrating dipalmitoylphosphatidylcholine multibilayers and reversed micelles. J Mol Struct 322:93–102
Guo Y, Yui H, Minamikawa H et al (2005) FT-IR study of the interlamellar water confined in glycolipid nanotube walls. Langmuir 21:4610–4614
Hansen FY, Peters GH, Taub H, Miskowiec A (2012) Diffusion of water and selected atoms in DMPC lipid bilayer membranes. J Chem Phys 137:204910
Harrick NJ (1987) Internal reflection spectroscopy, 3rd edn. Harrick Scientific Corporation, New York
Higgins MJ, Polcik M, Fukuma T et al (2006) Structured water layers adjacent to biological membranes. Biophys J 91:2532–2542
Hishida M, Tanaka K (2011) Long-range hydration effect of lipid membrane studied by terahertz time-domain spectroscopy. Phys Rev Lett 106:158102
Hodzic A, Rappolt M, Amenitsch H et al (2008) Differential modulation of membrane structure and fluctuations by plant sterols and cholesterol. Biophys J 94:3935–3944
Hübner W, Blume A (1998) Interactions at the lipid–water interface. Chem Phys Lipids 96:99–123
Ipsen JH, Karlström G, Mourtisen OG et al (1987) Phase equilibria in the phosphatidylcholine-cholesterol system. Biochim Biophys Acta Biomembr 905:162–172
Janiak M, Small D, Shipley G (1979) Temperature and compositional dependence of the structure of hydrated dimyristoyl lecithin. J Biol Chem 254:6068–6078
Jendrasiak G (1996) The hydration of phospholipids and its biological significance. J Nutr Biochem 7:599–609
Kasson PM, Lindahl E, Pande VS (2011) Water ordering at membrane interfaces controls fusion dynamics. J Am Chem Soc 133:3812–3815
Katsaras J (1997) Highly aligned lipid membrane systems in the physiologically relevant "excess water" condition. Biophys J 73:2924–2929
Kim J, Lu W, Qiu W et al (2006) Ultrafast hydration dynamics in the lipidic cubic phase: discrete water structures in nanochannels. J Phys Chem B 110:21994–22000
Kiselev M, Lesieur P, Kisselev A et al (1999) DMSO-induced dehydration of DPPC membranes studied by X-ray diffraction, small-angle neutron scattering, and calorimetry. J Alloys Compd 286:195–202
Kodama M, Aoki H, Takahashi H, Hatta I (1997) Interlamellar waters in dimyristoylphosphatidylethanolamine-water system as studied by calorimetry and X-ray diffraction. Biochim Biophys Acta 1329:61–73
Kodama M, Kato H, Aoki H (2001) Comparison of differently bound molecules in the gel and subgel phases of a phospholipid bilayer system. J Therm Anal Calorim 64:219–230
Kodama M, Kawasaki Y, Aoki H, Furukawa Y (2004) Components and fractions for differently bound water molecules of dipalmitoylphosphatidylcholine-water system as studied by DSC and ^{2}H-NMR spectroscopy. Biochim Biophys Acta 1667:56–66
Kucerka N, Liu Y, Chu N et al (2005) Structure of fully hydrated fluid phase DMPC and DLPC lipid bilayers using X-ray scattering from oriented multilamellar arrays and from unilamellar vesicles. Biophys J 88:2626–2637
Kuntz ID, Kauzmann W (1974) Hydration of proteins and polypeptides. Adv Protein Chem 28:239–345
Lafleur M, Pigeon M, Pezolet M, Caille J-P (1989) Raman spectrum of interstitial water in biological systems. J Phys Chem 93:1522–1526
Lefèvre T, Toscani S, Picquart M, Dugué J (2002) Crystallization of water in multilamellar vesicles. Eur Biophys J 31:126–135
Levinger N (2002) Water in confinement. Science 298:1722–1723
Lewis RNAH, McElhaney RN (2007) Fourier transform infrared spectroscopy in the study of lipid phase transitions in model and biological membranes: practical considerations. Methods Mol Biol 400:207–226
Libnau FO, Toft J, Christy AA, Kvalheim OM (1994) Structure of liquid water determined from infrared temperature profiling and evolutionary curve resolution. J Am Chem Soc 116:8311–8316

Lucent D, Vishal V, Pande VS (2007) Protein folding under confinement: a role for solvent. Proc Natl Acad Sci U S A 104:10430–10434

Mallikarjunaiah KJ, Leftin A, Kinnun JJ et al (2011) Solid-state ^{2}H NMR shows equivalence of dehydration and osmotic pressures in lipid membrane deformation. Biophys J 100:98–107

Manciu M, Ruckenstein E (2007) On possible microscopic origins of the swelling of neutral lipid bilayers induced by simple salts. J Colloid Interface Sci 309:56–67

Mantsch H (1984) Biological applications of Fourier transform infrared spectroscopy: a study of phase transitions in biomembranes. J Mol Struct 113:201–212

Mantsch HH, McElhaney RN (1991) Phospholipid phase transitions in model and biological membranes as studied by infrared spectroscopy. Chem Phys Lipids 57:213–226

Maréchal Y (1991) Infrared spectra of water. I. Effect of temperature and of H/D isotopic dilution. J Chem Phys 95:5565–5573

Marinov R, Dufourc E (1996) Thermotropism and hydration properties of POPE and POPE-cholesterol systems as revealed by solid state ^{2}H and 31P-NMR. Eur Biophys J 24:423–431

Markova N, Sparr E, Wadsö L, Wennerström H (2000) A calorimetric study of phospholipid hydration. Simultaneous monitoring of enthalpy and free energy. J Phys Chem B 104:8053–8060

McIntosh TJ, Simon SA (1986) Hydration force and bilayer deformation: a reevaluation. Biochemistry 25:4058–4066

McIntosh T, Simon S (1994) Hydration and steric pressures between phospholipid bilayers. Annu Rev Biophys Biomol Struct 23:27–51

McIntosh TJ, Simon SA (1996) Adhesion between phosphatidylethanolamine bilayers. Langmuir 12:1622–1630

Mennicke U, Salditt T (2002) Preparation of solid-supported lipid bilayers by spin-coating. Langmuir 18:8172–8177

Milhaud J (2004) New insights into water-phospholipid model membrane interactions. Biochim Biophys Acta 1663:19–51

Miller IR, Bach D (1999) Hydration of phosphatidyl serine multilayers and its modulation by conformational change induced by correlated electrostatic interaction. Bioelectrochem Bioenerg 48:361–367

Mills M, Orr BG, Banaszak Holl MM, Andricioaei I (2013) Attractive hydration forces in DNA-dendrimer interactions on the nanometer scale. J Phys Chem B 117:973–981

Murzyn K, Zhao W, Karttunen M et al (2006) Dynamics of water at membrane surfaces: effect of headgroup structure. Biointerphases 1:98–105

Nagle J, Katsaras J (1999) Absence of a vestigial vapor pressure paradox. Phys Rev E 59:7018–7024

Nagle JF, Tristram-Nagle S (2000) Structure of lipid bilayers. Biochim Biophys Acta Rev Biomembr 1469:159–195

Némethy G, Scheraga HA (1964) Structure of water and hydrophobic bonding in proteins. IV. The thermodynamic properties of liquid deuterium oxide. J Chem Phys 41:680–689

Okamura E, Umemura J, Takenaka T (1990) Orientation studies of hydrated dipalmitoylphosphatidylcholine multibilayers by polarized FTIR-ATR spectroscopy. Biochim Biophys Acta 1025:94–98

Omta AW, Kropman MF, Woutersen S, Bakker HJ (2003) Influence of ions on the hydrogen-bond structure in liquid water. J Chem Phys 119:12457–12461

Pandit SA, Bostick D, Berkowitz ML (2003) An algorithm to describe molecular scale rugged surfaces and its application to the study of a water/lipid bilayer interface. J Chem Phys 119:2199–2205

Parasassi T, De Stasio G, Ravagnan G et al (1991) Quantitation of lipid phases in phospholipid vesicles by the generalized polarization of Laurdan fluorescence. Biophys J 60:179–189

Paré C, Lafleur M (1998) Polymorphism of POPE/cholesterol system: a ^{2}H nuclear magnetic resonance and infrared spectroscopic investigation. Biophys J 74:899–909

Parsegian VA, Zemb T (2011) Hydration forces: observations, explanations, expectations, questions. Curr Opin Colloid Interface Sci 16:618–624

Parsegian V, Rand R, Fuller N, Rau D (1986) Osmotic stress for the direct measurement of intermolecular forces. Methods Enzymol 127:400–416

Pasenkiewicz-Gierula M, Takaoka Y, Miyagawa H et al (1997) Hydrogen bonding of water to phosphatidylcholine in the membrane as studied by a molecular dynamics simulation: location, geometry, and lipid-lipid bridging via hydrogen-bonded water. J Phys Chem A 101:3677–3691

Petrache H, Gouliaev N, Tristram-Nagle S et al (1998a) Interbilayer interactions from high-resolution x-ray scattering. Phys Rev E 57:7014–7024

Petrache HI, Tristram-Nagle S, Nagle JF (1998b) Fluid phase structure of EPC and DMPC bilayers. Chem Phys Lipids 95:83–94

Pfeiffer H, Klose G, Heremans K (2013) Reorientation of hydration water during the thermotropic main phase transition of 1-palmitoyl-2-oleolyl-sn-glycero-3-phosphocholine (POPC) bilayers at low degrees of hydration. Chem Phys Lett 572:120–124

Piletic IR, Moilanen DE, Levinger NE, Fayer MD (2006) What nonlinear-IR experiments can tell you about water that the IR spectrum cannot. J Am Chem Soc 128:10366–10367

Pinnick ER, Erramilli S, Wang F (2010) Computational investigation of lipid hydration water of L α 1-palmitoyl-2-oleoyl- sn -glycero-3-phosphocholine at three hydration levels. Mol Phys 108:2027–2036

Pohle W, Selle C (1996) Fourier-transform infrared spectroscopic evidence for a novel lyotropic phase transition occurring in dioleoylphosphatidylethanolamine. Chem Phys Lipids 82:191–198

Pohle W, Selle C, Fritzsche H, Bohl M (1997) Comparative FTIR spectroscopic study upon the hydration of lecithins and cephalins. J Mol Struct 408–409:273–277

Pohle W, Selle C, Fritzsche H, Binder H (1998) Fourier transform infrared spectroscopy as a probe for the study of the hydration of lipid self assemblies. I. Methodology and general phenomena. Biospectroscopy 4:267–280

Pohle W, Selle C, Gauger DR, Brandenburg K (2001) Lyotropic phase transitions in phospholipids as evidenced by small-angle synchrotron X-ray scattering. J Biomol Struct Dyn 19:351–364

Rand RP, Fuller NL (1994) Structural dimensions and their changes in a reentrant hexagonal-lamellar transition of phospholipids. Biophys J 66:2127–2138

Rand RP, Parsegian VA (1989) Hydration forces between phospholipid bilayers. Biochim Biophys Acta Rev Biomembr 988:351–376

Rand RP, Fuller N, Parsegian VA, Rau DC (1988) Variation in hydration forces between neutral phospholipid bilayers: evidence for hydration attraction. Biochemistry 27:7711–7722

Rappolt M, Hickel A, Bringezu F, Lohner K (2003) Mechanism of the lamellar/inverse hexagonal phase transition examined by high resolution x-ray diffraction. Biophys J 84:3111–3122

Riemenschneider J, Holzmann J, Ludwig R (2008) Salt effects on the structure of water probed by attenuated total reflection infrared spectroscopy and molecular dynamics simulations. Chemphyschem 9:2731–2736

Róg T, Murzyn K, Milhaud J et al (2009) Water isotope effect on the phosphatidylcholine bilayer properties: a molecular dynamics simulation study. J Phys Chem B 113:2378–2387

Selle C, Pohle W (1998) Fourier transform infrared spectroscopy as a probe for the study of the hydration of lipid self-assemblies. II. Water binding versus phase transitions. Biospectroscopy 4:281–294

Selle C, Pohle W, Fritzsche H (1999) FTIR spectroscopic features of lyotropically induced phase transitions in phospholipid model membranes. J Mol Struct 480–481:401–405

Sheikh KH, Jarvis SP (2011) Crystalline hydration structure at the membrane-fluid interface of model lipid rafts indicates a highly reactive boundary region. J Am Chem Soc 133:18296–18303

Skinner JL, Auer BM, Lin YS (2009) Vibrational line shapes, spectral diffusion, and hydrogen bonding in liquid water. Adv Chem Phys 142:59–103

Sokołowska A, Kęcki Z (1986) Inter- and intra-molecular coupling and Fermi resonance in the Raman spectra of liquid water. J Raman Spectrosc 17:29–33

Sovago M, Campen RK, Wurpel GWH et al (2008) Vibrational response of hydrogen-bonded interfacial water is dominated by intramolecular coupling. Phys Rev Lett 100:173901

Stepniewski M, Bunker A, Pasenkiewicz-Gierula M et al (2010) Effects of the lipid bilayer phase state on the water membrane interface. J Phys Chem B 114:11784–11792

Štrancar J, Arsov Z (2008) Application of spin-labeling EPR and ATR-FTIR spectroscopies to the study of membrane heterogeneity. In: Leitmannova Liu A (ed) Advances in planar lipid bilayers and liposomes, vol 6. Elsevier, Amsterdam, pp 16–139

Tamm LK, Han X (2000) Viral fusion peptides: a tool set to disrupt and connect biological membranes. Biosci Rep 20:501–518

Tamm LK, Tatulian SA (1997) Infrared spectroscopy of proteins and peptides in lipid bilayers. Q Rev Biophys 30:365–429

Tayebi L, Ma Y, Vashaee D et al (2012) Long-range interlayer alignment of intralayer domains in stacked lipid bilayers. Nat Mater 11:1074–1080

Ter-Minassian-Saraga L, Okamura E, Umemura J, Takenaka T (1988) Fourier transform infrared-attenuated total reflection spectroscopy of hydration of dimyristoylphosphatidyl-choline multi-bilayers. Biochim Biophys Acta 946:417–423

Tielrooij KJ, Paparo D, Piatkowski L et al (2009) Dielectric relaxation dynamics of water in model membranes probed by terahertz spectroscopy. Biophys J 97:2484–2492

Tiwari S, Ando M, Hamaguchi H (2013) Investigation of organelle-specific intracellular water structures with Raman microspectroscopy. J Raman Spectrosc 44:167–169

Tristram-Nagle S, Liu Y, Legleiter J, Nagle JF (2002) Structure of gel phase DMPC determined by X-ray diffraction. Biophys J 83:3324–3335

Volkov VV, Palmer DJ, Righini R (2007a) Heterogeneity of water at the phospholipid membrane interface. J Phys Chem B 111:1377–1383

Volkov VV, Palmer DJ, Righini R (2007b) Distinct water species confined at the interface of a phospholipid membrane. Phys Rev Lett 99:078302

Wennerström H, Sparr E (2003) Thermodynamics of membrane lipid hydration. Pure Appl Chem 75:905–912

Wurpel GWH, Müller M (2006) Water confined by lipid bilayers: a multiplex CARS study. Chem Phys Lett 425:336–341

Zhang Z, Berkowitz ML (2009) Orientational dynamics of water in phospholipid bilayers with different hydration levels. J Phys Chem B 113:7676–7680

Zhong D, Pal SK, Zewail AH (2011) Biological water: a critique. Chem Phys Lett 503:1–11